

## Article

# The Workability and Crack Resistance of Natural and Recycled Aggregate Mortar Based on Expansion Agent through an Environmental Study

Junfang Sun <sup>1</sup>, Ji Chen <sup>2</sup>, Xin Liao <sup>3,4,\*</sup>, Angran Tian <sup>2</sup>, Jinxu Hao <sup>5</sup>, Yuchen Wang <sup>6</sup> and Qiang Tang <sup>2</sup><sup>1</sup> Dongwu Business School, Soochow University, Suzhou 215021, China; jfsun@suda.edu.cn<sup>2</sup> School of Rail Transportation, Soochow University, Suzhou 215131, China;

20184246022@stu.suda.edu.cn (J.C.); gangguo@126.com (A.T.); tangqiang@suda.edu.cn (Q.T.)

<sup>3</sup> Faculty of Geoscience and Environmental Engineering, Southwest Jiaotong University, Chengdu 611756, China<sup>4</sup> MOE Key Laboratory of High-Speed Railway Engineering, Southwest Jiaotong University, Chengdu 611756, China<sup>5</sup> Suzhou Municipal Administrative Projects Management Office, Suzhou 215000, China; haojinxu@sina.com<sup>6</sup> Kogod School of Business, American University, Washington, DC 20016-8004, USA; yw7890a@student.american.edu

\* Correspondence: xinliao@swjtu.edu.cn; Tel.: +86-1388-007-4412

**Abstract:** Greenhouse gas emission has been a serious problem for decades. Due to the high energy consumption of traditional construction and building materials, recycled aggregate and other environmentally-friendly materials or recycled materials have been researched and applied. The treatment and reuse of construction and demolition waste (CDW) is a good way to reasonably distribute the renewable resources in the urban city. The recycled aggregate can be used in road engineering, geotechnical engineering and structural engineering. The combined use of natural aggregate and recycled aggregate may possess better performance in real constructions. This paper investigates the mechanical performance, micro-mechanism and CO<sub>2</sub> footprint assessment of NAM (natural aggregate mortar) and RAM (recycled aggregate mortar). Compressive strength test, flexural strength test, XRD and SEM, and CO<sub>2</sub> emission evaluation were conducted and analyzed. The results indicate that NAM depicts better compressive strength performance and RAM has higher flexural strength. The XRD and SEM patterns illustrate that the ettringite and C-S-H are the most important role in shrinkage-compensating mechanism, which is more obvious in RAM specimens. The proportion of CaO and MgO hydrated into Ca(OH)<sub>2</sub> and Mg(OH)<sub>2</sub> is also a key point of the volume expansion through the curing period. Finally, the CO<sub>2</sub> emission of NA is higher than RA per unit. This indicates that utilizing recycled aggregate over other conventional resources will reduce the energy consumption, and hit the mark to be environmental-friendly.

**Keywords:** recycled fine aggregate; expansion agent; mechanical properties; micro mechanism; carbon footprint



**Citation:** Sun, J.; Chen, J.; Liao, X.; Tian, A.; Hao, J.; Wang, Y.; Tang, Q. The Workability and Crack Resistance of Natural and Recycled Aggregate Mortar Based on Expansion Agent through an Environmental Study. *Sustainability* **2021**, *13*, 491. <https://doi.org/10.3390/su13020491>

Received: 14 December 2020

Accepted: 4 January 2021

Published: 6 January 2021

**Publisher's Note:** MDPI stays neutral with regard to jurisdictional claims in published maps and institutional affiliations.



**Copyright:** © 2021 by the authors. Licensee MDPI, Basel, Switzerland. This article is an open access article distributed under the terms and conditions of the Creative Commons Attribution (CC BY) license (<https://creativecommons.org/licenses/by/4.0/>).

## 1. Introduction

With the vigorous development of urban construction, a large number of old buildings and cement concrete pavement demolition and reconstruction have produced a huge amount of construction and demolition waste (CDW). By the end of 2020, the production of construction waste is expected to exceed three billion tons in China, while the resource utilization rate is only about 5%. With the acceleration of domestic development, the output of construction waste will continue to increase. Such a huge output of construction waste not only brings trouble to people's daily life, but also destroys the ecological environment. It will not only occupy a lot of land, but also destroy aquatic ecology [1–3].

Many developed countries have already regarded construction waste as a very rich resource, and the resource utilization rate of some countries has reached 100%. In most areas of China, construction waste is directly transported to the suburbs or rural waste dump without treatment, and then piled up or buried in the open air. Such simple and rough treatment of CDW will occupy land, polluting water, atmosphere and soil, thus damaging the ecological environment and endangering human life and health. In 2019, the total output of commercial concrete in China was 2.738 billion cubic meters [4–6]. However, 1700 to 2000 kg of aggregate can only produce 1 m<sup>3</sup> of concrete. Due to the huge demand for sand and gravel aggregate, a large number of woodlands have been destroyed, the environment has been destroyed and the ecological balance has been endangered. Excessive rock mining has caused serious damage to ecological landscape, frequent geological disasters and mine collapse [7,8].

Recycling of CDW will solve the problem of natural aggregate resources shortage. Also, it will solve the problems of random stacking of CDW, occupation of public land and environmental pollution. It can alleviate the social contradictions caused by construction waste, reduce the economic pressure for enterprises and protect the ecological environment effectively. It also presents a very far-reaching significance for the sustainable development of China's urbanization process and civil engineering industry [9,10]. Therefore, many countries are actively exploring how to recycle construction waste. At present, there are four ways to reuse construction waste: (1) to produce recycled aggregate; (2) to use for road cushion or subgrade filling; (3) for landscape engineering; (4) for foundation reinforcement. The recycling of construction waste to produce recycled aggregate can not only achieve better economic benefits, but also save a lot of natural aggregate, reduce the environmental damage caused by quarrying and achieve remarkable ecological benefits [11,12].

Many researches have analyzed the feasibility of recycled aggregate (RA) replacing natural aggregate (NA), or the combined use of RA and NA. The properties are relevant and similar, but also with some differences. As one kind of environmental-friendly material, the life cycle assessment (LCA) of RA is widely studied, and the emission of greenhouse gases are also be calculated and evaluated [13–15]. This paper investigates the mechanical performance, micro-mechanism and CO<sub>2</sub> footprint assessment of NAM (Natural aggregate mortar) and RAM (Recycled aggregate mortar). A series of compressive strength test, flexural strength test, XRD and SEM, and CO<sub>2</sub> emission evaluation were conducted. The purpose is to compare NA with RA, by analyzing the mechanical, micro and environmental performance.

## 2. Materials and Methods

### 2.1. Materials

#### 2.1.1. Aggregate

Both types of fine aggregate used in this paper were obtained in Suzhou, China. The river sand in Suzhou was used as natural aggregate (NA) and the recycled aggregate was prepared by construction and demolition waste from China Railway Tenth Group of The Fifth Engineering Co., Ltd. The particle size of these two kinds of aggregate after sieving was less than 4.75 mm, and the fineness modulus of NA and RA were 2.8 and 2.9 respectively. Figure 1a is the NA while Figure 1b represents RA.



(a) Natural Aggregate (NA)



(b) Recycled Aggregate (RA)

**Figure 1.** Aggregate.

### 2.1.2. Portland Cement and Expansion Agent

In this paper, Portland cement was used with the 7d compressive strength of 33.1 MPa and the 28d compressive strength of 46.2 MPa. The 7d and 28d flexural strength of Portland cement are 5.3 MPa and 8.1 MPa, respectively. Furthermore, the expansion agent (EXP) was supplied from Jiangsu SBT New Materials Co., Ltd., Suzhou, China. The chemical composition of Portland cement and EXP are shown in Table 1.

**Table 1.** Chemical composition of Portland cement and the expansion agent (EXP).

Composition	Na <sub>2</sub> O	SO <sub>3</sub>	SiO <sub>2</sub>	Fe <sub>2</sub> O <sub>3</sub>	Al <sub>2</sub> O <sub>3</sub>	MgO	CaO	K <sub>2</sub> O
Portland cement	0.20	4.34	22.75	2.61	7.92	2.02	51.91	0.93
Expansion agent	0.15	27.16	1.24	0.67	12.61	2.06	54.38	0.63

## 2.2. Methods

### 2.2.1. Specimen Preparations

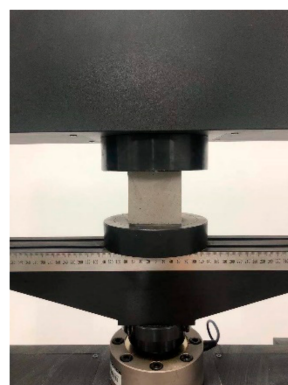
The tests were primarily regarding mechanical properties and micro-mechanism. Finally, the calculation of carbon emission aimed to compare recycled mortar and traditional materials based on the actual value of environmental-friendly materials.

The specimens of mechanical tests were all prepared under the curing temperature of  $20 \pm 2$  °C, and the humidity of mortar specimens curing condition was 95%. In this paper, the water-cement ratio was 0.45, and the mass ratio of aggregate to cement was almost 2.5. The NAM and RAM specimens were mainly composed of 0% EXP, 4.5% EXP, 9% EXP, 13.5% EXP and 18% EXP, with three parallel specimens in each mix proportion group. In the mixing procedure according to the standards, the mortar was mixed thoroughly by a cement-mortar mixer. The aggregate was added into the machine, and stirred in slow-speed mode for two minutes, then in high-speed mode for two minutes. Additionally, the percent of EXP was the mass ratio of EXP and cementitious material (Cement paste) [16].

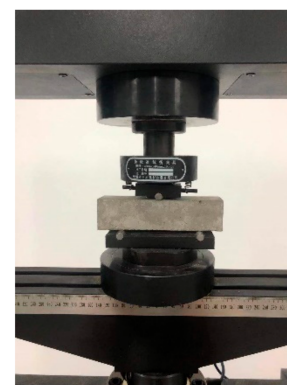
### 2.2.2. Compressive Strength Test

The size of the specimen was 70.7 mm × 70.7 mm × 70.7 mm, and the test device was a pressure testing machine CMT5305D with measuring range of 500 kN, as shown in Figure 2a. The loading pressure in the compressive strength test was 0.05 mm/min. The load and position at the time of damage were recorded through the test. The compressive strength is calculated as follows:

$$f_{m,cu} = K \times \frac{N_u}{A} \quad (1)$$



(a) Compressive strength test



(b) Flexural strength test

**Figure 2.** Mechanical tests.

In Formula (1),  $f_{m,cu}$  is the compressive strength of specimen (MPa),  $N_u$  is the damage pressure and K is conversion factor, which is 1.35 as used in this test.

### 2.2.3. Flexural Strength Test

In this test, the size of the specimen was 40 mm × 40 mm × 160 mm, and the test device was a pressure testing machine with measuring range of 300 kN, as shown in Figure 2b. The flexural test was carried out continuously at the loading speed of 0.01 mm/min until the test block was broken. The load and position at the time of damage were recorded through the test. The flexural strength is calculated as below:

$$f_b = \frac{3PL}{2bh^2} \quad (2)$$

In this formula,  $f_b$  is flexural strength of mortar (MPa),  $P$  is the loading pressure,  $L$  is the gap between supporting points, and  $b$  and  $h$  are the width and height of specimen section (mm), respectively [17].

### 2.2.4. Microscopic Mechanism Test

In order to investigate the different microscope performance between NAM and RAM, scanning electron microscope (SEM) and X-ray diffraction (XRD) were used. Also, the expansion mechanism of expansive agent needed to be considered from the microscopic view. In this part, the specimens were prepared and cured for 28 days before SEM and XRD tests.

### 2.2.5. Carbon Footprint Assessment

The environmental protection of recycled aggregate is supposed to be studied relative to CO<sub>2</sub> emission. In this paper, the carbon emissions of NAM and RAM per unit of cement were calculated and compared. CO<sub>2</sub> emission was calculated step by step from material demolition, process transportation and recycled aggregate production to quantify greenhouse gas CO<sub>2</sub> pollution systematically. The CO<sub>2</sub> emission system for the NAM and RAM production is depicted in Figure 3.

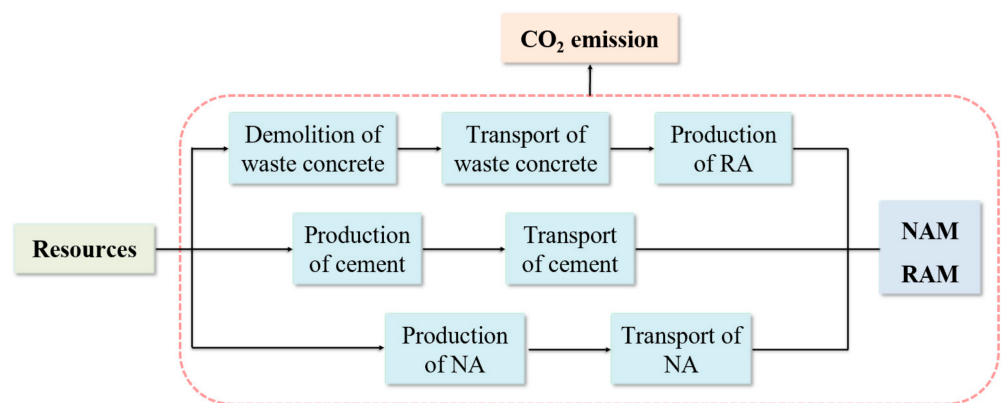


**Figure 3.** CO<sub>2</sub> emission system for the NAM and RAM production.

In the actual calculation process, it is difficult to get the accurate data of aggregate and cement production enterprises or data in actual transportation process. Therefore, the carbon emission coefficient method was used to estimate and compare the carbon emission of recycled aggregate and natural aggregate in the process of production, transportation and usage. The carbon emission of the material can be obtained by multiplying the consumption or output in the production, transportation and mixing ratio of NAM and RAM in Figure 3 by the corresponding unit carbon emission coefficient, as shown in Formula (3) [18–20].

$$Q_1 = N_1 I_1 \quad (3)$$

Formula (4) is obtained by combining the carbon emissions of all materials:

$$\sum Q = \sum_{i=1}^n N_i I_i \quad (4)$$

In this formula,  $Q$  is the whole CO<sub>2</sub> emission,  $N$  is the quantity of material and  $I$  represent carbon emission per unit of material. Table 2 illustrates the carbon emission coefficient.

**Table 2.** Carbon emission coefficient.

Coefficient (/t)	Factor $I$	Unit
Cement	0.8	t
Diesel	3.16	kg
Electricity	1.0	kg
RA	Electricity: 1.20 kW/t; Diesel: 0.73 L/t 3.22	kg
NA	Electricity: 1.50 kW/t; Diesel: 0.80 L/t 3.66	kg
Water	0.53	kg
Mixture	0.012	kg

The mix proportion of NAM and RAM is shown in Table 3. Other components were ignored in this part and we only took water, cement and NA/RA into consideration [21–23].

**Table 3.** Mix proportion.

Material	Water	Cement	NA/RA
Proportion/t	0.150	0.271	1

### 3. Results and Discussion

#### 3.1. Compressive Strength and Flexural Strength

##### 3.1.1. Compressive Strength

The effect of expansive agent on the strength of NAM is shown in Figure 4. In Figure 4a, the 7d compressive strength of mortar with 9% EXP content is the highest of all groups of specimens. It can be seen that the maximum 28d compressive strength of the specimen is almost 6 MPa higher than that of the original specimen. However, too much expansive agent reduces the compressive strength. The initial strength of cement is the lowest when the content of EXP reaches 18%.

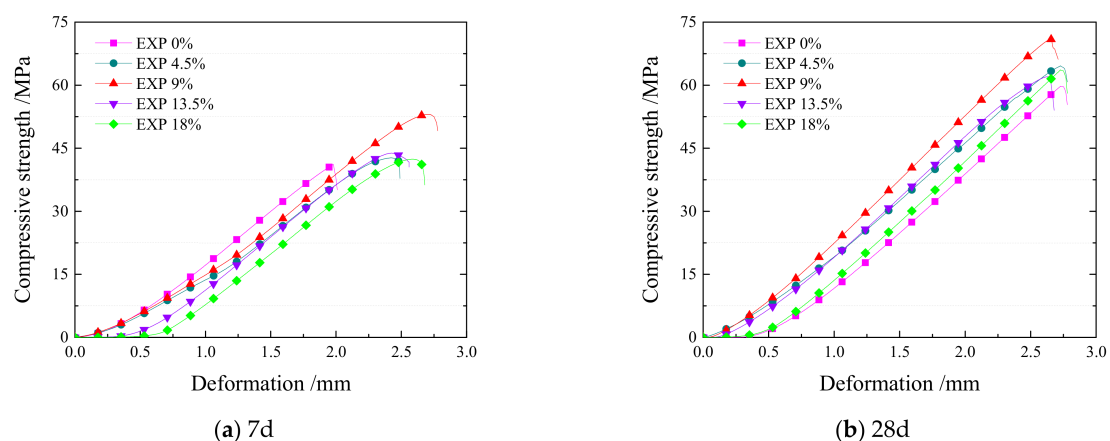


**Figure 4.** Compressive strength of NAM.

When the proportion of EXP increases, the compressive strength rises, reaches the peak at 9%, and decreases with a relatively big value. It seems that the EXP enhances the early age compressive strength and the max deformation range, which means that the mortar possesses much higher crack resistance. As a result, there is less possibility for cracks to emerge in the early stage [24,25].

The recycled aggregate completely replaces the natural aggregate to make mortar specimens in this paper. As shown in Figure 5, the content of EXP has a great influence on the 7d compressive strength of RAM, whereas it has little effect on the 28d compressive strength. In Figure 5a, the compressive strength of 9% EXP is the highest, and the ultimate displacement is the same as that of 18% EXP. Compared with NAM, the early age strength decreases, and the maximum strength is only 46.5 MPa, which is about 3 MPa lower than RAM. Compared with NAM, the displacement of 7d specimen is less than 0.3 mm, which means that the ultimate deformation capacity of early age RAM is kinds of weak. The deformation resistance of RAM is similar to that of NAM when the curing time reaches 28d. The compressive strength curve of 28d RAM specimens is shown in Figure 5b, and the effect of expansion agent content on the compressive strength of specimens is relatively small. The strength difference of several groups is little, while 9% EXP content is still the optimal content.

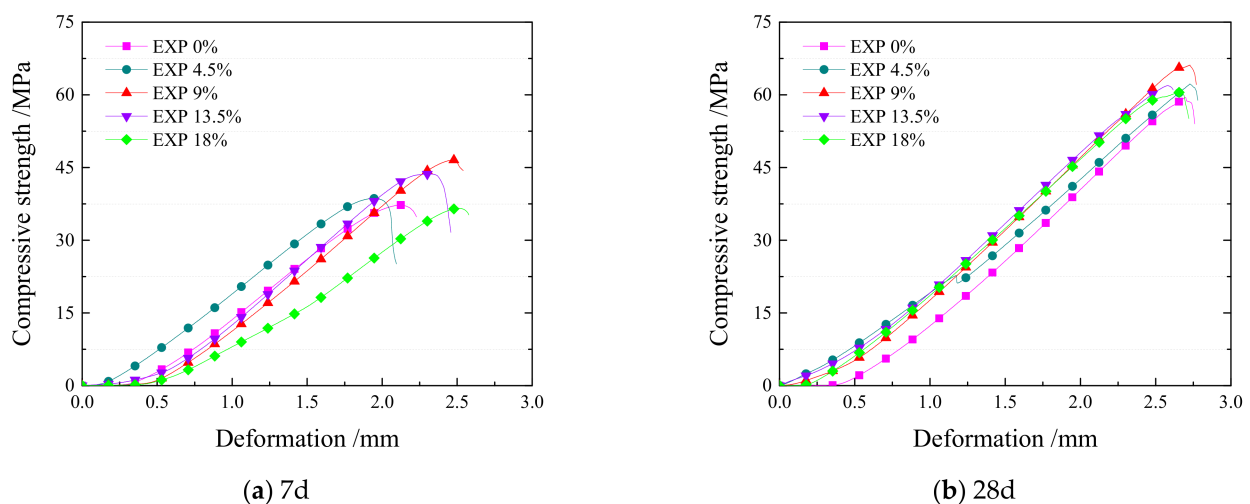


Figure 5. Compressive strength of RAM.

Compared with NAM, the strength is 4 MPa less. Because the recycled aggregate is a kind of environmental material and a new saving type for secondary utilization, its internal compound composition is relatively stable. Therefore, under the effect of additives, the bond strength of cement after hydration is not obvious. That is also the reason why RAM compressive strength is not higher than NAM, replaced by the considerably stable value.

### 3.1.2. Flexural Strength

The original data of flexural strength test has been simplified and present in Figures 6 and 7. Figure 6 depicts the flexural strength of NAM. The changing trend of flexural strength is similar to compressive strength of NAM. The flexural strength first increases, then decreases when the proportion of EXP reaches 13.5%. The max 7d flexural strength is almost 7.6 MPa, while the 28d flexural strength is about 9.2 MPa at the EXP content of 9% and 13.5%. However, the deformation is quite different as to 7d flexural strength. When the proportion is around 9%, the ultimate deformation is the biggest, which means that the EXP increase the crack resistance of specimens and the plasticity is improved from specimens of 0% EXP [26,27].

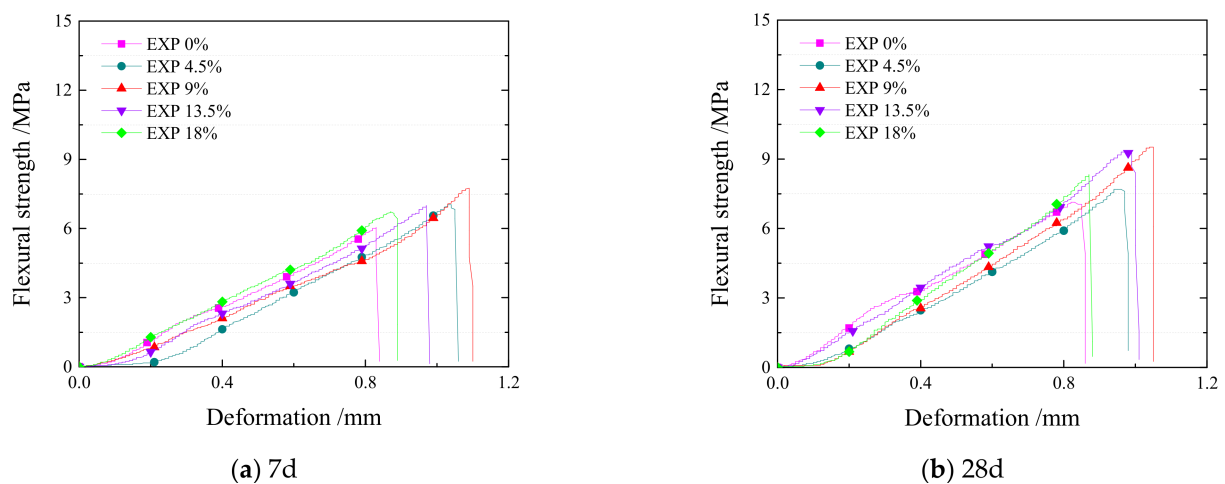


Figure 6. Flexural strength of NAM.

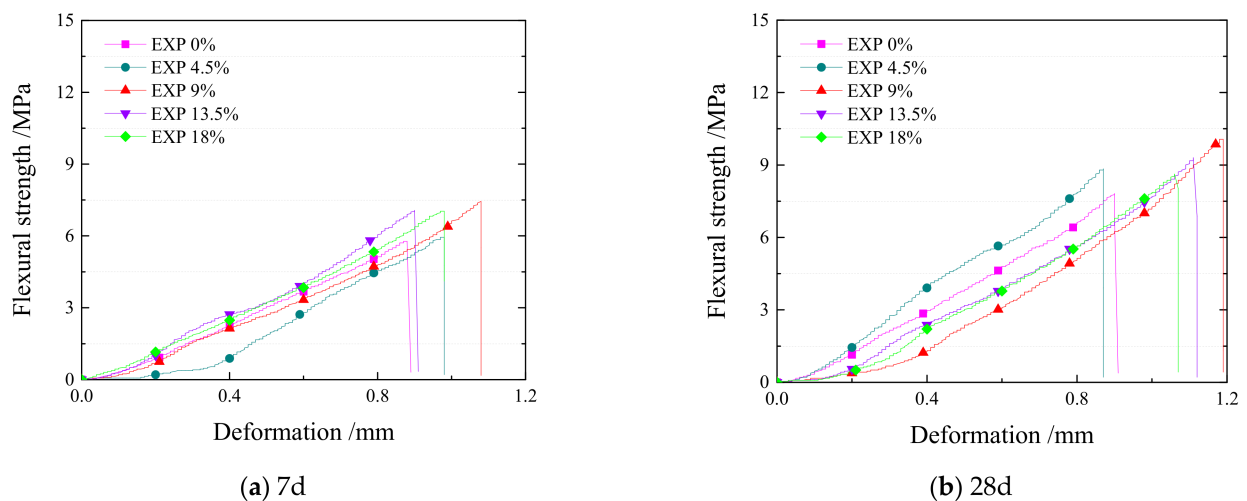


Figure 7. Flexural strength of RAM.

Compared with NAM flexural strength, the strength value of RAM is different. The biggest distinct between NAM and RAM is the deformation. In Figure 7a, the max flexural strength is 7.5 MPa and the changing range is relatively small, similar to compressive strength of RAM in Figure 5. The 28d flexural strength of RAM is higher than NAM, with a difference of approximately 0.3 MPa. However, the ultimate strain of RAM is 1.2 mm, while that of NAM is only around 1.03 mm. With the content of 9%, the specimens present better plasticity.

Combining the compressive strength and flexural strength, the effect of EXP exposed on NAM is much obvious than RAM. Above all, the strength performance of NAM is a little bit better than RAM, and the strength of RAM is much stable than NAM. The flexural strength of RAM is higher than NAM, which means that RAM has better performance under bending force. On the other words, NAM possesses higher crack-resistance under compressive strength [28,29].

Pictures of some specimens after the test are collected, as shown in Figure 8. The development of cracks in compressive strength specimens starts from one third of one side of the specimen. The bubbles on the surface of NAM specimens are obviously less than those of RAM specimens, which is related to the particle size and fineness modulus of RAM. Also, the RAM absorbs more water than NAM and reduces the mixing water, which generates more porosity in the samples. The failure modes of the bending specimens are consistent, and all fracture from the middle of the specimens. The addition of EXP limits

the initial volume expansion of cement water and compensates the volume shrinkage during curing and cooling. It can be seen from the above results that EXP has more obvious compensation shrinkage mechanism in NAM specimens. At the end of the curing period, the strength enhancement plays an important role. For RAM, the effect of EXP is limited to the secondary utilization of aggregate, so the effect is not so obvious [30,31].

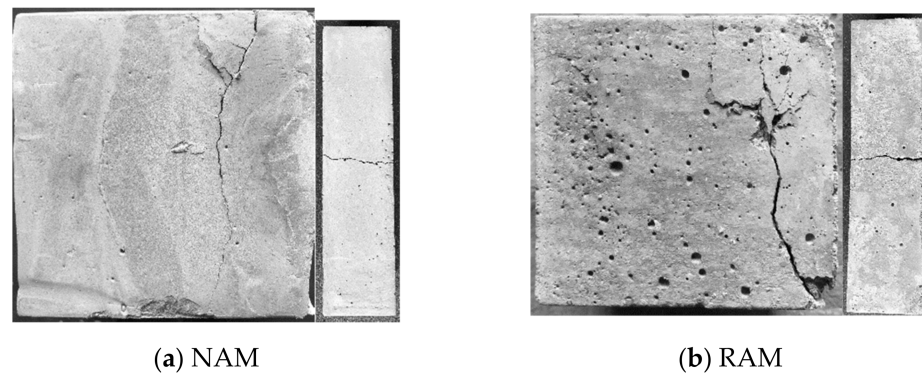


**Figure 8.** Failure mode.

### 3.2. X-Ray Diffraction (XRD) and Scanning Electron Microscope (SEM)

#### 3.2.1. X-Ray Diffraction (XRD)

Figure 9 shows the XRD chemical composition pattern of NAM with 0% EXP and 9% EXP, and of RAM with 9% EXP. The strength of mortar and concrete is mainly from quartz. The quartz content of RAM is less than NAM, which is the main reason why the strength of RAM is lower than that of NAM. Due to the utilization of CDW, the components of RAM are more complex, as shown in Figure 9.

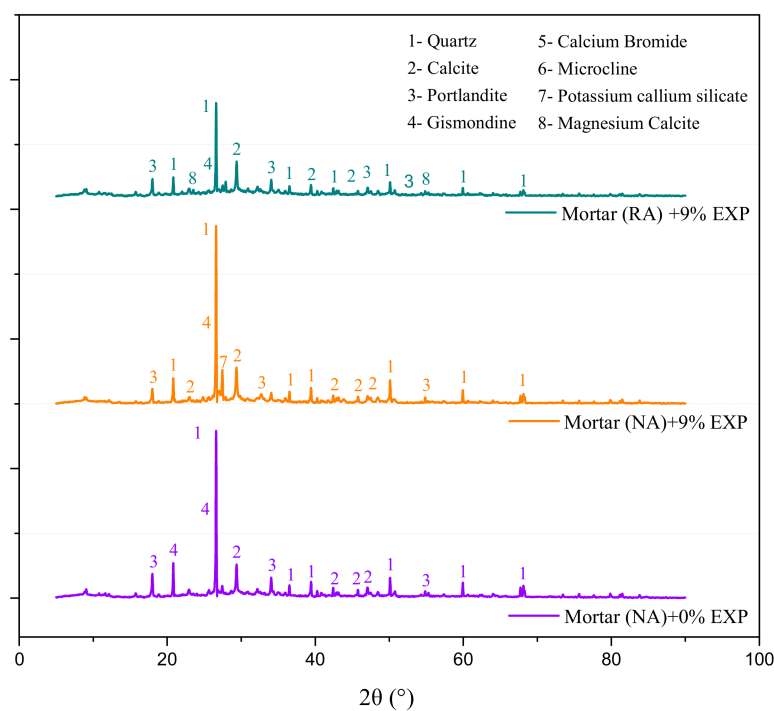


**Figure 9.** XRD pattern.

There are many reasons that may explain the shrinkage compensating mechanism of EXP used in RAM and NAM. Firstly, the EXP cement which forms ettringite occurs in the early stage of cement hydration, as shown in Formula (1). It is suitable for function in

lower temperature under 60 °C. The solid volume of the system increases by almost 120% before and after the reaction [32–34].



Furthermore, the hydration of CaO or MgO in the EXP forms  $\text{Ca}(\text{OH})_2$  or  $\text{Mg}(\text{OH})_2$ , resulting in volume expansion. The solid volume increases by 98% when CaO is hydrated to  $\text{Ca}(\text{OH})_2$ , and about 117% when MgO is hydrated to  $\text{Mg}(\text{OH})_2$ . Therefore, that's the difference between the three mortar specimens below. EXP has the function of shrinkage-compensation and it changes both the chemical composition and the mechanical performance.

### 3.2.2. Scanning Electron Microscope (SEM)

Compared with SEM images of NAM, the microstructure of RAM is loose, as shown in Figure 10. The hydration products contain more C-S-H in NAM and ettringite (needle shape), and less large crystals. At the same time, a large number of calcium hydroxide crystals overlap each other. This is consistent with RAM having lower strength and NAM having better performance.

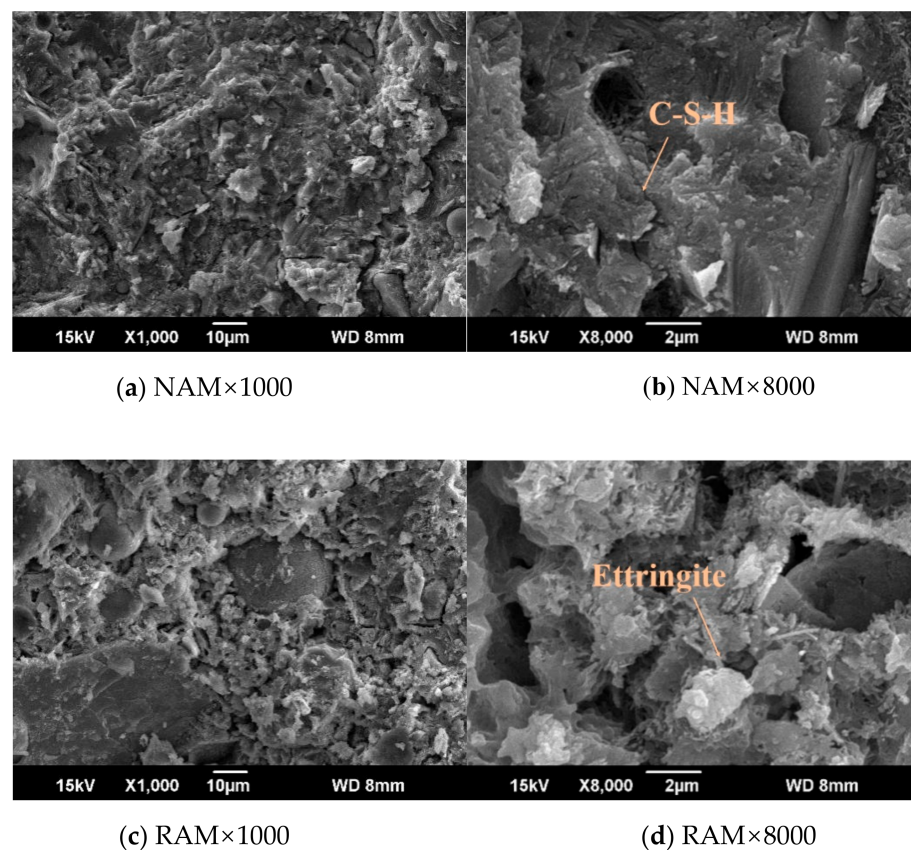


Figure 10. SEM images of NAM and RAM.

Ettringite is adsorbed on the crystal to form clusters. When the mortar is cured in early age, the internal temperature rises and the mortar volume expands. However, the excessive expansion is limited by ettringite. During the curing period, the internal temperature drops and the volume shrinkage leads to the obvious internal shrinkage stress. The shrinkage strain can easily lead to the formation of micro cracks. In this stage, C-S-H and ettringite play an important role in compensating volume shrinkage and minimizing internal deformation. The same principle is also applied to crack and impermeable concrete [35–37].

### 3.3. Carbon Emission Evaluation

Based on the data above, the CO<sub>2</sub> emission of NAM and RAM through the cycle of material can be calculated. The CO<sub>2</sub> emission proportion of different components is illustrated in Table 4.

**Table 4.** CO<sub>2</sub> emission proportion/%.

NAM	Production and Transport of Cement		Production and Transport of NA	Mixture
	96.02		3.57	0.41
RAM	Demolition of waste concrete	Production and Transport of Cement	Production and Transport of RA	Mixture
	1.44	94.67	3.55	0.34

In the cycle of RAM and NAM production, the proportion of production and transport of cement occupies around 94% to 96% of total CO<sub>2</sub> emission. It seems that the CO<sub>2</sub> emission of RAM is a little bit less than NAM, mainly because the production and transport of RA saves diesel and electricity consumption. As a result, the utilization of recycled aggregate from CDW or other environmental-friendly resources may reduce the energy use; at the same time, the greenhouse gas will also be controlled to some extent. Last but not least, the NA and RA can be combined in actual use to obtain better performance. A reasonable proportion of NA or RA in concrete mixing, casting and laying will realize higher strength and resistance, and also meet environmental targets [38–40].

## 4. Conclusions

In this paper, the aggregate is fine aggregate. The natural aggregate and recycled aggregate, combined with the utilization of expansion agent, were investigated and discussed based on mechanical performance, micro-mechanism and environmental evaluation. Various tests, including compressive strength test, flexural strength test, XRD, SEM and CO<sub>2</sub> emission evaluation, were conducted. The conclusions are drawn as below:

1. The compressive strength of NAM is higher than that of RAM, while the flexural strength of NAM is less than RAM. Further, the trend of mechanical strength is similar in that it first increases and then decreases when the EXP proportion reaches an optimal level. The strength value of recycled aggregate is acceptable compared with that of NAM.
2. From the XRD and SEM patterns, quartz is the source of strength in NAM and RAM. Ettringite occurs in the early stage of cement hydration and C-S-H are the main courses of shrinkage-compensating mechanism. At the same time, the CaO and MgO may be hydrated to Ca(OH)<sub>2</sub> and Mg(OH)<sub>2</sub>, and the volume relatively expanded. The effect of EXP on NAM and RAM is similar, and it has significant influence.
3. The proportion of production and transport of cement occupies around 94% to 96% of CO<sub>2</sub> emission. The CO<sub>2</sub> emission of RAM is a little bit less than NAM; as a result, the utilization of recycled aggregate from CDW or other environmental-friendly resources may reduce the energy consumption.

**Author Contributions:** Conceptualization: J.S. and Q.T.; methodology: J.S. and J.C.; validation, J.C. and A.T.; formal analysis: J.S., X.L. and J.H.; investigation: J.C., X.L. and J.S.; resources: J.S. and J.C.; data curation: J.C., Y.W., A.T. and J.H.; writing—original draft preparation: J.S., J.C. and A.T.; writing—review and editing: J.S., J.C., X.L., A.T. and Y.W.; supervision: Q.T., X.L. and J.C.; project administration: J.S. and Q.T. All authors have read and agreed to the published version of the manuscript.

**Funding:** The research presented here is supported by the National Nature Science Foundation of China (52078317), Natural Science Foundation of Jiangsu Province (BK20170339), project from Jiangsu Provincial Department of Housing and Urban-Rural Development (2020ZD05), and Bureau of Housing and Urban-Rural Development of Suzhou (2020-15).

**Institutional Review Board Statement:** Not applicable.

**Informed Consent Statement:** Not applicable.

**Data Availability Statement:** The research data supporting this publication are given within this paper.

**Conflicts of Interest:** The authors declare no conflict of interest.

## References

- Chinzorigt, G.; Choi, D.; Enkhbold, O.; Baasankhuu, B.; Lim, M.K.; Lim, H.S. Strength, shrinkage and creep of concrete including CO<sub>2</sub> treated recycled coarse aggregate. *J. Asian Concr. Fed.* **2018**, *4*, 89–102. [[CrossRef](#)]
- Corinaldesi, V. Combined effect of expansive, shrinkage reducing and hydrophobic admixtures for durable self-compacting concrete. *Constr. Build. Mater.* **2012**, *36*, 758–764. [[CrossRef](#)]
- Zhao, R.; Su, H.; Chen, X.L.; Yu, Y.N. Commercially available materials selection in sustainable design: An integrated multi-attribute decision making approach. *Sustainability* **2016**, *8*, 79. [[CrossRef](#)]
- Kua, H.W.; Gupta, S.; Aday, A.N.; Srubar, W.V. Biocharimmobilized bacteria and superabsorbent polymers enable self-healing of fiber-reinforced concrete after multiple damage cycles. *Cem. Concr. Compos.* **2019**, *100*, 35–52. [[CrossRef](#)]
- Tang, Q.; Zhang, Y.; Gao, Y.F.; Gu, F. Use of cement-chelated solidified MSWI fly ash for pavement material: Mechanical and environmental evaluations. *Can. Geotech. J.* **2017**, *54*, 1553–1566. [[CrossRef](#)]
- Tang, Q.; Liu, Y.; Gu, F.; Zhou, T. Solidification/stabilization of fly ash from a municipal solid waste incineration facility using Portland cement. *Adv. Mater. Sci. Eng.* **2016**, *5*, 1–10. [[CrossRef](#)]
- Tang, Q.; Gu, F.; Gao, Y. Desorption characteristics of Cr (III), Mn (II) and Ni (II) in contaminated soil using citric acid and citric acid containing wastewater. *Soils Found.* **2018**, *58*, 5–64.
- Tang, Q.; Tang, X.W.; Li, Z.Z. Zn (II) removal with activated Firmiana simplex leaf: Kinetics and equilibrium studies. *J. Environ. Eng.* **2012**, *138*, 190–199. [[CrossRef](#)]
- Zhao, R.; Li, M.; Ma, S.D.; Yang, T.X.; Jing, L.Y. Material selection for landfill leachate piping by using a grey target decision-making approach. *Environ. Sci. Pollut. Res.* **2020**, 1–9. [[CrossRef](#)]
- Zhao, R.; Wang, X.Q.; Chen, X.L.; Liu, Y.Y. Impacts of different aged landfill leachate on PVC corrosion. *Environ. Sci. Pollut. Res.* **2019**, *26*, 18256–18266. [[CrossRef](#)]
- Shahidan, S.; Rahim, M.A.; Zol, N.S.N.; Azizan, M.A.; Ismail, I. Properties of steel fibers reinforcement concrete with different characteristic of steel fiber. *Appl. Mech. Mater.* **2015**, *5*, 773–774. [[CrossRef](#)]
- Shen, D.; Liu, K.; Wen, C.; Shen, Y.; Jiang, G. Early-age cracking resistance of ground granulated blast furnace slag concrete. *Constr. Build. Mater.* **2019**, *222*, 278–287. [[CrossRef](#)]
- Zhao, R.; Xi, B.D.; Liu, Y.Y.; Su, J.; Liu, S.L. Economic potential of leachate evaporation by using landfill gas: A system dynamics approach. *Resour. Conserv. Recycl.* **2017**, *124*, 74–84. [[CrossRef](#)]
- Zhao, R.; Zhou, X.; Han, J.J.; Liu, C.L. For the sustainable performance of the carbon reduction labeling policies under an evolutionary game simulation. *Technol. Forecast. Soc. Chang.* **2016**, *112*, 262–274. [[CrossRef](#)]
- Zhao, R.; Liu, Y.Y.; Zhang, N.; Huang, T. An optimization model for green supply chain management by using a big data analytic approach. *J. Clean. Prod.* **2017**, *142*, 1085–1097. [[CrossRef](#)]
- Liu, S.; Fang, K.; Li, Z. Influence of Mineral Admixtures on Crack Resistance of High Strength Concrete. *Key Eng. Mater.* **2006**, *302*, 150–154. [[CrossRef](#)]
- Calvo, J.L.C.; Revuelta, D.; Carballosa, P.; Gutierrez, J.P. Comparison between the performance of expansive SCC and expansive conventional concretes in different expansion and curing conditions. *Constr. Build. Mater.* **2017**, *136*, 277–285. [[CrossRef](#)]
- Lee, S.; Park, W.; Lee, H. Life cycle CO<sub>2</sub> assessment method for concrete using CO<sub>2</sub> balance and suggestion to decrease CO<sub>2</sub> of concrete in South-Korean apartment. *Energy Build.* **2013**, *58*, 93–102. [[CrossRef](#)]
- Han, Y.; Wu, Y.; Zhao, X. Life cycle assessment of heavy-duty truck for highway transport in China. *Mater. Sci. Forum* **2014**, *787*, 117–122.
- Li, C.; Cui, S.; Nie, Z.; Gong, X.; Wang, Z.; Itsubo, N. The LCA of Portland cement production in China. *Int. J. Life Cycle Assess.* **2015**, *20*, 117–127. [[CrossRef](#)]
- Gong, X.; Nie, Z.; Wang, Z.; Cui, S.; Gao, F.; Zuo, T. Life cycle energy consumption and carbon dioxide emission of residential building designs in Beijing. *J. Ind. Ecol.* **2012**, *16*, 576–587. [[CrossRef](#)]
- Tam, C.M.; Tsui, W.S. Green construction assessment for environmental management in the construction industry of Hong Kong. *Int. J. Proj. Manag.* **2004**, *22*, 563–571. [[CrossRef](#)]
- Xin, J.; Zhang, G.; Liu, Y.; Wang, Z.; Yang, N.; Wang, Y.; Mou, R.; Qiao, Y.; Wang, J.; Wu, Z. Environmental impact and thermal cracking resistance of low heat cement (LHC) and moderate heat cement (MHC) concrete at early ages. *J. Build. Eng.* **2020**, *32*, 101668. [[CrossRef](#)]
- Dulsang, N.; Kasemsiri, P.; Posi, P.; Hiziroglu, S.; Chindaprasirt, P. Characterization of an environment friendly lightweight concrete containing ethyl vinyl acetate waste. *Mater. Des.* **2016**, *96*, 350–356. [[CrossRef](#)]
- Nežerka, V.; Havlásek, P.; Trejbal, J. Mitigating inclusion-induced shrinkage cracking in cementitious composites by incorporating recycled concrete fines. *Constr. Build. Mater.* **2020**, *248*, 118673. [[CrossRef](#)]

26. Meddah, M.S.; Tagnit-Hamou, A. Evaluation of rate of deformation for early age concrete shrinkage analysis and time zero determination. *J. Mater. Civ. Eng.* **2011**, *23*, 1076–1086. [[CrossRef](#)]
27. Marsavina, L.; Audenaert, K.; De Schutter, G.; Faur, N.; Marsavina, D. Experimental and numerical determination of the chloride penetration in cracked concrete. *Constr. Build. Mater.* **2009**, *23*, 264–274. [[CrossRef](#)]
28. Marinkovic, S.; Radonjanin, V.; Malesev, M.; Ignjatovic, I. Comparative environmental assessment of natural and recycled aggregate concrete. *Waste Manag.* **2010**, *30*, 2255–2264. [[CrossRef](#)]
29. Thilakarathna, P.S.M.; Seo, S.; Baduge, K.S.K.; Lee, H.; Mendis, P.; Foliente, G. Embodied carbon analysis and benchmarking emissions of high and ultra-high strength concrete using machine learning algorithms. *J. Clean. Prod.* **2020**, *262*, 121281. [[CrossRef](#)]
30. Tang, Q.; Tang, X.W.; Li, Z.Z. Adsorption and desorption behaviour of Pb (II) on a natural kaolin: Equilibrium, kinetic and thermodynamic studies. *J. Chem. Technol. Biotechnol.* **2009**, *84*, 1371–1380. [[CrossRef](#)]
31. Bravo, M.; de Brito, J.; Evangelista, L.; Pacheco, J. Superplasticizer's efficiency on the mechanical properties of recycled aggregates concrete: Influence of recycled aggregates composition and incorporation ratio. *Constr. Build. Mater.* **2017**, *153*, 129–138. [[CrossRef](#)]
32. Pereira, P.; Evangelista, L.; de Brito, J. The effect of superplasticizers on the mechanical performance of concrete made with fine recycled concrete aggregates. *Cem. Concr. Compos.* **2012**, *34*, 1044–1052. [[CrossRef](#)]
33. Burgos-Montes, O.; Palacios, M.; Rivilla, P.; Puertas, F. Compatibility between superplasticizer admixtures and cements with mineral additions. *Constr. Build. Mater.* **2012**, *31*, 300–309. [[CrossRef](#)]
34. Tan, H.; Zou, F.; Liu, M.; Ma, B. Effect of the adsorbing behavior of phosphate retarders on hydration of cement paste. *J. Mater. Civ. Eng.* **2017**, *29*, 04017088. [[CrossRef](#)]
35. Zhan, M.; Pan, G.; Wang, Y.; Fu, M.; Lu, X. Effect of presoak- accelerated carbonation factors on enhancing recycled aggregate mortars. *Mag. Concr. Res.* **2017**, *69*, 838–849. [[CrossRef](#)]
36. Chau, C.; Hui, W.; Ng, W.; Powell, G. Assessment of CO<sub>2</sub> emissions reduction in high-rise concrete office buildings using different material use options. *Resour. Conserv. Recycl.* **2012**, *61*, 22–34. [[CrossRef](#)]
37. Asutosh, A.; Nawari, N.O. Integration of recycled industrial wastes into pavement design and construction for a sustainable future. *J. Sustain. Dev.* **2017**, *10*, 9–23. [[CrossRef](#)]
38. De Schepper, M.; Van den Heede, P.; Van Driessche, I.; De Belie, N. Life cycle assessment of completely recyclable concrete. *Materials* **2014**, *7*, 6010–6027. [[CrossRef](#)]
39. Xiao, J.; Ma, Z.; Sui, T.; Akbarnezhad, A.; Duan, Z. Mechanical properties of concrete mixed with recycled powder produced from construction and demolish waste. *J. Clean. Prod.* **2018**, *188*, 720–731. [[CrossRef](#)]
40. Hossain, U.; Xuan, D.; Poon, C.S. Sustainable management and utilization of concrete slurry waste: A case study in Hong Kong. *Waste Manag.* **2017**, *61*, 397–404. [[CrossRef](#)]